in vivo *35*: 921-927 (2021)
doi:10.21873/invivo.12332

Diagnostic Utility of Oncomine Comprehensive Assay v3 in Differentiating Between Isocitrate Dehydrogenase (IDH)-mutated Grade II-III Astrocytoma and Oligodendroglioma

SO-WOON KIM[1], BONG JIN PARK[2], HYUN-SOO KIM[3] and KIYONG NA[1]

[1]*Department of Pathology, Kyung Hee University Hospital, Kyung Hee University College of Medicine, Seoul, Republic of Korea;*
[2]*Department of Neurosurgery, Kyung Hee University Hospital, Kyung Hee University College of Medicine, Seoul, Republic of Korea;*
[3]*Department of Pathology and Translational Genomics, Samsung Medical Center, Sungkyunkwan University School of Medicine, Seoul, Republic of Korea*

Abstract. *Background/Aim: The application of Oncomine Comprehensive Assay v3 (OCAv3) panel in diffuse gliomas (DGs) remains unknown. We investigated the utility of OCAv3-based next-generation sequencing (NGS) in isocitrate dehydrogenase (IDH)-mutated grade II-III DGs. Patients and Methods: We collected 20 tissue samples obtained from IDH-mutated grade II-III DG patients and performed OCAv3-based NGS. Results: By conventional molecular methods, the 20 DGs were classified into seven astrocytomas and 13 oligodendrogliomas. OCAv3 detected all mutations identified in these samples using the conventional methods. The results were highly corroborated by the known mutations in each group. Clustered copy number loss of genes located at the 1p and 19q loci was detected in all 13 oligodendroglioma cases, which harbor the 1p/19q codeletion. Conclusion: The application of OCAv3-based NGS will improve diagnostic accuracy in DG, with the most beneficial aspects expected in detecting copy number alterations to identify the 1p/19q codeletion correctly.*

Correspondence to: Kiyong Na, Department of Pathology, Kyung Hee University Hospital, Kyung Hee University College of Medicine, 26, Kyungheedae-ro, Dongdaemun-gu, Seoul 02447, Republic of Korea. Tel: +82 29588740, Fax: +82 29588744, e-mail: raripapa@gmail.com; Hyun-Soo Kim, Department of Pathology and Translational Genomics, Samsung Medical Center, Sungkyunkwan University School of Medicine, 81, Irwon-ro, Gangnam-gu, Seoul 06351, Republic of Korea. Tel: +82 234101243, Fax: +82 234132831, e-mail: hyun-soo.kim@samsung.com

Key Words: Glioma, astrocytoma, oligodendroglioma, next-generation sequencing, Oncomine Comprehensive Assay v3.

Diffuse glioma (DG) is the largest group of primary malignant central nervous system (CNS) tumors in adults (1). According to the 2016 World Health Organization (WHO) Classification (2), DGs include grade II-III astrocytomas (AC), grade II-III oligodendrogliomas (OD), and grade IV glioblastomas, as well as the related DGs in children and young adults. The current WHO Classification recommends molecular subtyping of DGs in addition to histological diagnosis, using an appropriate testing for the isocitrate dehydrogenase (*IDH)* mutation and further genetic alterations associated with the *IDH* mutational status (3). However, the conventional molecular subtyping of *IDH*-mutated grade II-III DGs requires a time- and material-consuming multistep approach, including 1p/19q fluorescence *in situ* hybridization (FISH) and telomerase reverse transcriptase (*TERT)* promoter sequencing. Moreover, the results obtained from these molecular techniques may show equivocal findings. In such cases, detection of other genetic mutations characteristically occurring in AC and OD can support the precise molecular subtyping.

Next-generation sequencing (NGS) is a useful approach for the analysis of high-yield genes or genomic regions, with a fairly fast turnaround time, low DNA input, and low cost (4). While several targeted NGS panels are available commercially, most of them are designed to cover the important alterations detected in carcinomas and do not target gliomas specifically. The Oncomine Comprehensive Assay panel v3 (OCAv3, Thermo Fisher Scientific, Waltham, MA, USA) consists of a DNA workflow for the identification of relevant single-nucleotide variants, amplification, small insertions and deletions, copy number variation, and a panel of 161 genes for the identification of gene fusions (5, 6). To the best of our knowledge, the application of the OCAv3 to DGs has not been reported yet. In this study, we applied the OCAv3 panel-based NGS

technique to 20 tissue samples obtained from *IDH*-mutated grade II-III DG patients and evaluated its utility in the context of establishing a one-step analysis system for their differential diagnosis.

Patients and Methods

Case selection. This study (2020-03-081) was reviewed and approved by the Institutional Review Board of Kyung Hee University Hospital (Seoul, Republic of Korea). We found 65 cases of grade II-III DG in the surgical pathology database of the Department of Pathology at Kyung Hee University Hospital (Seoul, Republic of Korea), using the following keywords: i) diffuse AC, ii) anaplastic AC, iii) OD, and iv) anaplastic OD. The tissue specimens were obtained by surgical biopsy or resection between January 2007 and December 2019. All clinical data were retrieved from the electronic medical records.

Pathological examination. All available hematoxylin and eosin-stained slides were reviewed by two board-certified pathologists. Both of them selected the most representative slide to perform IDH1-R132H immunostaining, 1p/19q FISH, *TERT* promoter sequencing, and NGS.

Immunohistochemistry. The Bond Polymer Intense Detection System (Vision Biosystems, Mount Waverly, Victoria, Australia) was used according to the manufacturer's instructions with minor modifications (7-19). Four-micrometer-thick formalin-fixed, paraffin-embedded (FFPE) tissue sections were deparaffinized, antigen-retrieved, and then incubated for 15 minutes at ambient temperature with a mouse monoclonal antibody against IDH1-R132H (dilution 1:100, Clone H09, Dianova, Hamburg, Germany). The nuclei were counterstained with hematoxylin. A negative control was prepared by substituting the primary antibody with a non-immune serum sample, which resulted in no detectable staining.

Nucleic acid extraction. Five-micrometer-thick FFPE sections were deparaffinized in xylene and hydrated through graded alcohols to water. The slides were manually microdissected using a scalpel point dipped in ethanol. The scraped material was washed in phosphate-buffered saline and digested in proteinase K overnight at 56˚C in Buffer ATL (Qiagen, Hilden, Germany). DNA and RNA were then isolated using a QIAamp DSP DNA FFPE Tissue Kit (Qiagen) according to the manufacturer's instructions (15-17). A Qubit 4 Fluorometer (Thermo Fisher Scientific) was used for sample quantitation by means of the highly sensitive and accurate fluorescence-based quantitation assays.

TERT promoter sequencing. Two hotspot mutations in the *TERT* core promoter, C228T and C250T, correspond to positions 124- and 146-bp upstream of the ATG site. Polymerase chain reaction (PCR) was performed in a 30 μl reaction containing 100 ng template DNA, 10× PCR buffer, 0.25 mM dNTPs, 10 pmol primers, and 1.25 U Taq DNA polymerase (Solgent, Daejeon, Republic of Korea). The amplification protocol was 35 cycles at 94˚C for 45 s, 55˚C for 45 s, and 72˚C for 45 s, and one cycle at 72˚C for 5 min. The PCR products were subjected to electrophoresis on 2% agarose gels and purified with a QIAquick PCR Purification Kit (Qiagen). Bidirectional sequencing was performed using a BigDye Terminator v1.1 Cycle Sequencing Kit (Applied Biosystems, Foster City, CA, USA) on an ABI 3130XL Genetic Analyzer (Applied Biosystems). The results were regarded as mutation-positive if a mutation was detected in both forward and reverse read directions. We used Sequencher v4.10.1 (Gene Codes Corporation, Ann Arbor, MI, USA), together with a manual review of the chromatograms.

Dual-color locus-specific FISH. We used probes targeting 1p36/1q25 and 19q13/19p13 (ZytoLight Glioma 1p/19q Probe Set, ZytoVision, Bremerhaven, Germany). All probe pairs were co-denatured with the tissue sections and hybridized overnight at 37˚C in separate slides. After hybridization, the slides were washed with 2× saline-sodium citrate/ 0.1% nonyl phenoxypolyethoxylethanol for 2 min at 73˚C, counterstained with 4,6-diamidino-2-phenylindole dihydrochloride, and then cover-slipped. The proportion of nuclei containing only one signal of 1p or 19q was calculated, with more than 60 nuclei possessing two centromeric signals evaluated. Deletion was defined as a signal ratio of more than 50% for the region of interest to control the probe.

NGS and variant analysis. NGS library preparation for the OCAv3 (Thermo Fisher Scientific) using extracted DNA and RNA was performed using the Ion AmpliSeq Library Preparation on the IonChef System protocol (Thermo Fisher Scientific). Sequencing was performed on the IonTorrent S5 XL platform, following manufacturer's instructions and using positive control cell line mixtures (Horizon Discovery, Cambridge, UK). The OCAv3 is an amplicon-based, targeted assay that enables the detection of relevant single-nucleotide variants, amplifications, gene fusions, and indels from 161 unique genes. Genomic data were analyzed and alterations were detected using the IonReporter Software v5.6 (Thermo Fisher Scientific). We also manually reviewed the variant call format file and integrated genomic viewer. Only variants in coding regions, promoter regions, or splice variants were retained. All genes subject to copy number analysis were sorted by their chromosomal loci and the mean copy number of each gene was documented.

Statistical analysis. Mann–Whitney *U*-tests were used to compare the means between continuous variables. Statistical analyses were performed using an IBM SPSS Statistics for Windows, v22.0 (IBM Corp., Armonk, NY). Statistical significance was set at $p<0.05$.

Results

Patient demographics. Twenty-three of the 65 DGs exhibited at least focal positivity for IDH1-R132H, whereas in the remaining 42 cases IDH1-R132H expression was absent. The patients whose tumors showed positive IDH1-R132H expression (mean age=41.9 years) were significantly younger compared to those with IDH1-R132H-negative tumors (mean age=52.1 years, $p=0.009$). Male to female ratios were 1.3 (male: female=13:10) and 2.0 (male: female=28:14) for IDH1-R132H-positive and -negative cases, respectively.

Conventional integrated diagnosis of IDH-mutated DGs. The vast majority (40/42, 95.2%) of IDH1-R132H-negative DGs displayed astrocytic histology. In contrast, 23 IDH1-R132H-positive tumors showed a relatively even distribution of the predominant histological features: i) nine (39.1%) cases were

oligodendroglial, ii) eight (34.8%) were astrocytic, and iii) six (26.1%) were oligoastrocytic. To generate integrated diagnoses, 20 of the 23 cases showing appropriate tissue quality and quantity were further examined using *TERT* promoter sequencing, 1p/19q FISH, and NGS. Three IDH1-R132H-positive tumors with astrocytic features were excluded from the molecular analyses due to low quantity and quality of the DNA.

The diagnoses were established according to both the 2016 WHO Classification and the updated series from the Consortium to Inform Molecular and Practical Approaches to CNS Tumor Taxonomy-Not Official WHO (cIMPACT-NOW) (20). Among the 20 tumors examined, five (62.5%) tumors with astrocytic features and two (33.3%) tumors with oligoastrocytic features showed wildtype *TERT* promoter region and intact 1p/19q, indicating that these seven cases harboring neither *TERT* promoter mutation nor 1p/19q codeletion are compatible with grade II-III *IDH*-mutant AC. In contrast, the remaining 13 cases showed *TERT* promoter mutations and 1p/19q codeletion, indicating that nine (100.0%) tumors with oligodendroglial features and four (66.7%) tumors with oligoastrocytic features harboring both genetic abnormalities are compatible with grade II-III *IDH*-mutant OD.

Single-nucleotide variants and indels detected by NGS. Overall, 96.4% of the targeted sequences had at least 1,800× target base coverage across the samples. The exonic variants detected by the IonReporter Software (Thermo Fisher Scientific) and manual review were concordant in all 20 cases examined. The mutational analyses of the exonic region revealed 40 DNA sequence changes, including 31 missense mutations, 6 truncating mutations, and 3 in-frame deletions.

The mean depths of coverage in four hot spots of the *TERT* promoter region extracted from the 20 cases were 125.1 (g.1295228), 167.3 (g.1295229), 164.5 (g.1295242), and 161.3 (g.1295250), respectively. Despite the low read depth, the results of a manual review were consistent with those of *TERT* promoter sequencing (mutation-positive in 13 sets and wildtype in 7 sets). The results of *TERT* promoter-wildtype cases were concordant between *TERT* promoter sequencing and NGS; however, in 7 of the 13 mutation-positive cases, the IonReporter Software did not detect any mutation in *TERT* promoter region.

Figure 1 demonstrates the mutational profiles detected by OCAv3. All 20 tumors exhibited *IDH1* mutations in the form of R132H. In seven ACs, tumor protein 53 (*TP53*) mutations (6/7, 85.7%) were the most common genetic alteration, followed by ATP-dependent helicase chromatin remodeler (*ATRX*) mutations (3/7, 42.9%). In 13 ODs, *TERT* promoter mutations were detected as C228T (11/13, 84.6%) and C250T (2/13, 15.4%). A small subset of ODs was found to harbor mutations in: i) phosphoinositide-3-kinase regulatory subunit 1 (*PIK3R1*), ii) AT-rich interaction domain 1A (*ARID1A*), iii) notch homolog 1 (*NOTCH1*), iv) protein tyrosine phosphatase non-receptor type 11 (*PTPN11*), v) SET domain containing 2, vi) histone lysine methyltransferase (*SETD2*), and vii) splicing factor 3b subunit 1 (*SF3B1*).

Copy number variation detected by NGS. Figure 2A demonstrates the copy number values of 146 genes arranged by their chromosomal loci. In the mean copy number of 2.0, the relative copy number of each gene was calculated. We focused on the copy number of gene clusters in each chromosomal arm. The genes located at 1p and 19q were: i) notch homolog 2 (*NOTCH2*, 1p12p11.2), ii) neuroblastoma RAS viral oncogene homolog (*NRAS*, 1p13.2), iii) Janus kinase 1 (*JAK1*, 1p31.3), iv) v-myc avian myelocytomatosis viral oncogene homolog 1 (*MYCL1*, 1p34.2), v) *ARID1A* (1p36.11), vi) mammalian target of rapamycin (*MTOR*, 1p36.22), vii) cyclin E1 (*CCNE1*, 19q12), viii) anexelekto receptor tyrosine kinase (*AXL*, 19q13.2), ix) AKT serine/threonine kinase 2 (*AKT2*, 19q13.32), x) excision repair cross-complementing rodent repair deficiency, complementation group 2 (*ERCC2*, 19q13.32), and xi) protein phosphatase 2 scaffold subunit alpha (*PPP2R1A*, 19q13.41). In ODs, copy number variations in these genes were detected in less than 20% of the cases (range=5-20%), except for X chromosome genes in male patients. The mean copy number of these genes was 1.27. In ACs, the copy number of genes located at the 1p and 19q loci were distributed close to 2.0, with the mean value of 1.98 (range=48-73%). In grade II-III tumors, the mean copy numbers of these 1p ($p<0.001$; Figure 2B) and 19q ($p<0.001$; Figure 2C) loci in ODs were significantly lower than those in ACs. In both ACs and ODs, the clustering of genes occupying less than 10% of copy numbers was recurrently detected in 14p loci genes [MYC-associated factor X (*MAX*), RAD51 paralog B (*RAD51B*), and AKT serine/threonine kinase 1 (*AKT1*); two ODs and one AC], 9p loci genes [cyclin-dependent kinase inhibitor 2A (*CDKN2A*), cyclin-dependent kinase inhibitor 2 (*CDKN2B*), and Janus kinase 2 (*JAK2*); three ODs and three ACs], and X chromosomal genes (A-Raf proto-oncogene, serine/threonine kinase (*ARAF*), androgen receptor (*AR*), mediator complex subunit 12 (*MED12*), *ATRX*, and Bruton tyrosine kinase (*BTK*); all 13 male patients; Figure 2D). Several genes showed mildly increased copy numbers (range=4.1-4.5) but did not appear as clustering patterns in the same chromosomal loci.

Discussion

We analyzed the molecular features of 20 *IDH*-mutated grade II-III DGs using OCAv3-based NGS. Several considerations regarding targeted NGS assay should be noted. The panel

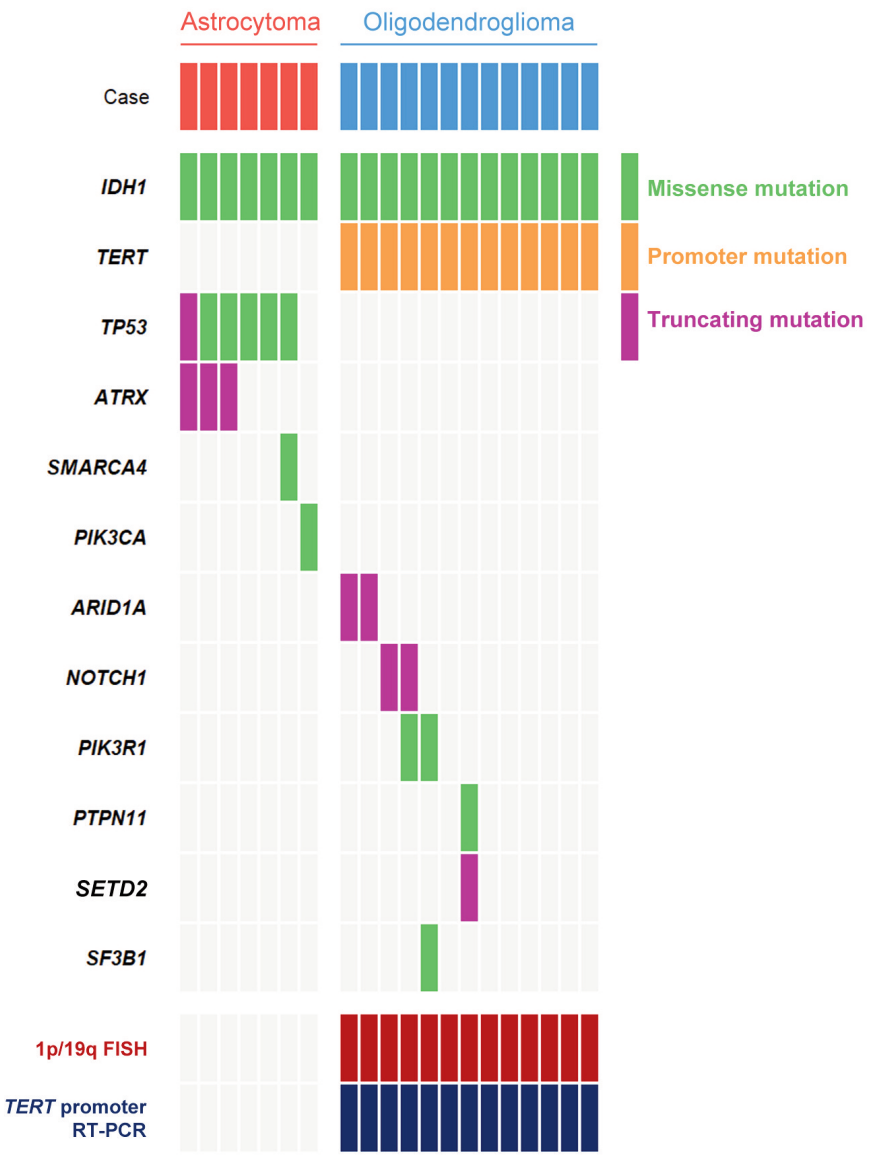

Figure 1. *Mutational profiles of 20 isocitrate dehydrogenase (IDH)-mutant diffuse gliomas detected by Oncomine Comprehensive Assay v3. TERT: Telomerase reverse transcriptase; TP53: tumor protein 53; ATRX: ATP-dependent helicase chromatin remodeler; SMARCA4: SWI/SNF-related, matrix associated, actin-dependent regulator of chromatin, subfamily A, member 4; PIK3CA: phosphatidylinositol-4,5-bisphosphate 3-kinase catalytic subunit alpha; ARID1A: AT-rich interaction domain 1A; NOTCH1: notch homolog 1; PIK3R1: phosphoinositide-3-kinase regulatory subunit 1; PTPN11: protein tyrosine phosphatase non-receptor type 11; SETD2: SET domain containing 2, histone lysine methyltransferase; SF3B1: splicing factor 3b subunit 1; FISH: fluorescence in situ hybridization; RT-PCR: reverse transcriptase-polymerase chain reaction.*

should cover a wide set of genes and their various types of genetic alterations, which may have diagnostic, therapeutic, predictive, and prognostic implications for the targeted tumors. Furthermore, the interpretation should show high reliability in FFPE tissues (5). The OCAv3-based NGS analysis revealed high sensitivity and demonstrated the detection of all mutations found in these samples by the conventional molecular methods. Of note, 1p/19q codeletion as determined by FISH was also detected by OCAv3-based NGS, through the loss of clustered copy number of genes located at the 1p/19q loci. In addition, the OCAv3 panel covers a wide set of diagnostically important genes, including *TERT*, *TP53*, and *ATRX*, which can help establish a precise diagnosis. These results suggest that OCAv3-based NGS, as a single analysis, can aid the pathologists in differentiating between *IDH*-mutant OD and AC.

There were some challenges associated with the detection of *TERT* promoter mutations. While all 13 ODs harbored *TERT* promoter mutations, the IonReporter Software

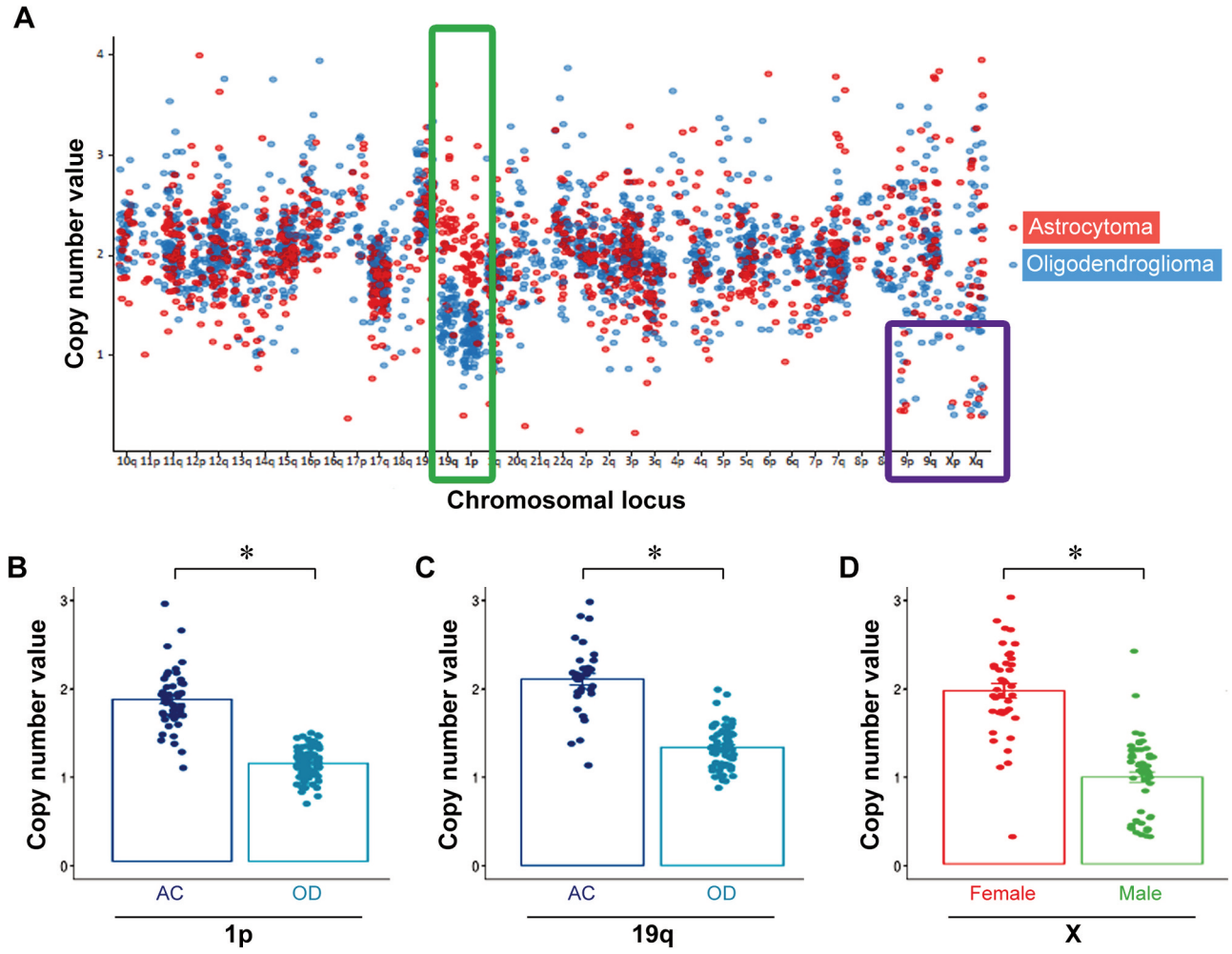

Figure 2. *Comparison of copy number values between isocitrate dehydrogenase (IDH)-mutant astrocytoma (AC) and oligodendroglioma (OD). (A) Overview of total copy number values of all chromosomal loci. The green box in A corresponds to significant decreases in copy number values of the (B) 1p and (C) 19q loci in OD. In both loci, the differences in the mean copy number values between IDH-mutant AC and OD are statistically significant. The purple box in A corresponds to copy number values in the (D) X-linked loci, as an internal control. Female patients have significantly higher copy number values in the X-linked loci genes compared to male patients. *p<0.001.*

detected the mutations in only half of OD cases. Some negative cases were needed to adjust the manual review of the NGS data. We considered that these false-negative results were mainly caused by the filtering out of the low-depth regions or strand bias in the software analysis. Therefore, a careful examination is crucial when false-negative results are found in the *TERT* promoter region, even though the tumors exhibit a typical histology of OD. Another limitation of the OCAv3 panel for the analysis of DGs was the composition of the target genes, which did not include some high-yield genes often mutated in ODs. The value of the OCAv3 for routine practice would be improved by including capicua transcriptional repressor (*CIC*) and far upstream element binding protein 1 (*FUBP1*) mutations, which frequently occur in ODs.

The incidences of *IDH* mutations and related results observed in our cases were mainly similar to those of previous studies (21). Two major classes of molecular profiles were noted in *IDH*-mutant DGs. Firstly, grade II-III AC has genetic alterations such as the *TP53* mutation and loss of *ATRX*. These findings indicate that *IDH*, *TP53*, and *ATRX* mutations occur as early events during AC pathogenesis and that tumors progress with the accumulation of additional events (22). Secondly, grade II-III ODs were categorized by a *TERT* mutation and 1p/19q codeletion status, whereas they lacked a *TP53* mutation and *ATRX* loss. In addition, *NOTCH1* and

ARID1A mutations were more often detected in OD than in AC, suggesting that previous studies have reported recurrent mutations of these genes in only a subset of ODs (23).

The genetic hallmark of OD is the complete loss of chromosome arms 1p and 19q, although approximately 20% of ODs are associated with incomplete 1p/19q-codeletion (24). Consistent with this data, in this study, the copy numbers of the 1p/19q genes in OD cases were significantly lower compared to those of AC cases. We observed similar differences in the comparison of copy number loss in X-linked gene loci between male and female patients, which originated from the different numbers of X chromosomes. We showed that copy number analysis may not show significant copy number losses for every single gene in the 1p/19q loci in OD cases. However, the overall decreasing pattern of these genes was in agreement with the FISH results, suggesting that clustered loss patterns are important when diagnosing OD. We recently demonstrated, using the TruSight Tumor 170 panel, that ODs have clustered copy number loss patterns in genes located at the 1p/19q loci (25). However, this panel included only two genes in 1p and four genes in 19q loci. As the OCAv3 included 11 genes located at the two loci, clustered copy number loss in these genes was more clearly visualized. In several cases, we observed recurrent clustered copy number loss patterns in 14q and 9p loci genes. Previous studies have reported copy number losses in 14q and 9p, with a frequency of 35% and 67%, respectively, in low-grade gliomas (26-28).

In conclusion, we reported the utility of the OCAv3 panel-based NGS assay for subtyping *IDH*-mutated DGs. The application of OCAv3 in clinical and laboratory settings showed diagnostic accuracy for differentiating between AC and OD. Particularly, the most beneficial aspects of this assay are expected in the detection of copy number alterations, including 1p/19q codeletion, correctly and indirectly, as well as the variable composition of a wide gene set.

Conflicts of Interest

The Authors declare that they have no conflicts of interest.

Authors' Contributions

All Authors made substantial contributions to the conception and design of the study; the acquisition, analysis, and interpretation of the data; drafting of the article; critical revision of the article for important intellectual content; and the final approval of the version to be published.

References

1 Goodenberger ML and Jenkins RB: Genetics of adult glioma. Cancer Genetics *205(12)*: 613-621, 2012. PMID: 23238284. DOI: 10.1016/j.cancergen.2012.10.009

2 Nikiforova MN, Wald AI, Melan MA, Roy S, Zhong S, Hamilton RL, Lieberman FS, Drappatz J, Amankulor NM, Pollack IF, Nikiforov YE and Horbinski C: Targeted next-generation sequencing panel (GlioSeq) provides comprehensive genetic profiling of central nervous system tumors. Neuro-Oncology *18(3)*: 379-387, 2015. PMID: 26681766. DOI: 10.1093/neuonc/nov289

3 Louis DN, Perry A, Reifenberger G, von Deimling A, Figarella-Branger D, Cavenee WK, Ohgaki H, Wiestler OD, Kleihues P and Ellison DW: The 2016 World Health Organization Classification of Tumors of the Central Nervous System: a summary. Acta Neuropathol *131(6)*: 803-820, 2016. PMID: 27157931. DOI: 10.1007/s00401-016-1545-1

4 Nikiforova MN, Wald AI, Roy S, Durso MB and Nikiforov YE: Targeted next-generation sequencing panel (ThyroSeq) for detection of mutations in thyroid cancer. J Clin Endocrinol Metab *98(11)*: E1852-E1860, 2013. PMID: 23979959. DOI: 10.1210/jc.2013-2292

5 Sakai K, Takeda M, Shimizu S, Takahama T, Yoshida T, Watanabe S, Iwasa T, Yonesaka K, Suzuki S, Hayashi H, Kawakami H, Nonagase Y, Tanaka K, Tsurutani J, Saigoh K, Ito A, Mitsudomi T, Nakagawa K and Nishio K: A comparative study of curated contents by knowledge-based curation system in cancer clinical sequencing. Sci Rep *9(1)*: 11340, 2019. PMID: 31383922. DOI: 10.1038/s41598-019-47673-9

6 Lih CJ, Harrington RD, Sims DJ, Harper KN, Bouk CH, Datta V, Yau J, Singh RR, Routbort MJ, Luthra R, Patel KP, Mantha GS, Krishnamurthy S, Ronski K, Walther Z, Finberg KE, Canosa S, Robinson H, Raymond A, Le LP, McShane LM, Polley EC, Conley BA, Doroshow JH, Iafrate AJ, Sklar JL, Hamilton SR and Williams PM: Analytical validation of the next-generation sequencing assay for a nationwide signal-finding clinical trial: Molecular Analysis for Therapy Choice clinical trial. J Mol Diagn *19(2)*: 313-327, 2017. PMID: 28188106. DOI: 10.1016/j.jmoldx.2016.10.007

7 Kim SW, Kim HS and Na K: Characterization of paired box 8 (PAX8)-expressing metastatic breast carcinoma. Anticancer Res *40(10)*: 5925-5932, 2020. PMID: 32988924. DOI: 10.21873/anticanres.14613

8 Bae GE, Yoon N, Cho EY, Kim HS and Cho SY: Clinicopathological and molecular characteristics of mammary adenoid cystic carcinoma with adipocytic differentiation with emphasis on the identification of a novel *BRAF* mutation. Anticancer Res *39(1)*: 369-374, 2019. PMID: 30591482. DOI: 10.21873/anticanres.13121

9 Jung YY, Woo HY and Kim HS: targeted genomic sequencing reveals novel *TP53* in-frame deletion mutations leading to p53 overexpression in high-grade serous tubo-ovarian carcinoma. Anticancer Res *39(6)*: 2883-2889, 2019. PMID: 31177126. DOI: 10.21873/anticanres.13417

10 Kim HG, Park MS, Sung JY, Kim YW, Kim HS and Na K: Tumor-specific expression of insulin-like growth factor II mRNA-binding protein 3 independently predicts worse survival of patients with adenocarcinoma of the ampulla of Vater. Anticancer Res *39(9)*: 4947-4955, 2019. PMID: 31519600. DOI: 10.21873/anticanres.13683

11 Kim HS, Do SI, Kim DH and Apple S: Clinicopathological and prognostic significance of programmed death ligand 1 expression in Korean patients with triple-negative breast carcinoma. Anticancer Res *40(3)*: 1487-1494, 2020. PMID: 32132048. DOI: 10.21873/anticanres.14093

12 Kim JY, Kim SH and Kim HS: Promoter methylation down-regulates osteoprotegerin expression in ovarian carcinoma. Anticancer Res *39(5)*: 2361-2367, 2019. PMID: 31092428. DOI: 10.21873/anticanres.13353
13 Kim SJ, Kim SW, Oh CH, Hong M, Do SI, Kim YW, Kim HS and Na K: Expression of insulin-like growth factor II mRNA-binding Protein 3 in gallbladder carcinoma. Anticancer Res *40(10)*: 5777-5785, 2020. PMID: 32988905. DOI: 10.21873/anticanres.14594
14 Park S, Cho EY, Oh YL, Park YH and Kim HS: Primary peritoneal high-grade serous carcinoma misinterpreted as metastatic breast carcinoma: a rare encounter in peritoneal fluid cytology. Anticancer Res *40(5)*: 2933-2939, 2020. PMID: 32366445. DOI: 10.21873/anticanres.14271
15 Jung H, Bae GE, Kim HM and Kim HS: Clinicopathological and molecular differences between gastric-type mucinous carcinoma and usual-type endocervical adenocarcinoma of the uterine cervix. Cancer Genomics Proteomics *17(5)*: 627-641, 2020. PMID: 32859641. DOI: 10.21873/cgp.20219
16 Kim H, Yoon N, Woo HY, Lee EJ, Do SI, Na K and Kim HS: Atypical mesonephric hyperplasia of the uterus harbors pathogenic mutation of kirsten rat sarcoma 2 viral oncogene homolog (*KRAS*) and gain of chromosome 1q. Cancer Genomics Proteomics *17(6)*: 813-826, 2020. PMID: 33099482. DOI: 10.21873/cgp.20235
17 Kim HN, Woo HY, Do SI and Kim HS: Targeted sequencing of tubo-ovarian and peritoneal high-grade serous carcinoma with wild-type p53 immunostaining pattern. In Vivo *33(5)*: 1485-1492, 2019. PMID: 31471396. DOI: 10.21873/invivo.11628
18 Kim M and Kim HS: Clinicopathological characteristics of well-differentiated papillary mesothelioma of the peritoneum: a single-institutional experience of 12 cases. In Vivo *33(2)*: 633-642, 2019. PMID: 30804152. DOI: 10.21873/invivo.11521
19 Park CK, Kim YW, Koh HH, Yoon N, Bae GE and Kim HS: Clinicopathological characteristics of squamous cell carcinoma and high-grade squamous intraepithelial lesions involving endocervical polyps. In Vivo *34(5)*: 2613-2621, 2020. PMID: 32871791. DOI: 10.21873/invivo.12079
20 Onizuka H, Masui K and Komori T: Diffuse gliomas to date and beyond 2016 WHO Classification of Tumours of the Central Nervous System. Int J Clin Oncol *25(6)*: 997-1003, 2020. PMID: 32468200. DOI: 10.1007/s10147-020-01695-w
21 Mukasa A, Takayanagi S, Saito K, Shibahara J, Tabei Y, Furuya K, Ide T, Narita Y, Nishikawa R, Ueki K and Saito N: Significance of *IDH* mutations varies with tumor histology, grade, and genetics in Japanese glioma patients. Cancer Sci *103(3)*: 587-592, 2012. PMID: 22136423. DOI: 10.1111/j.1349-7006.2011.02175.x
22 Carter JH, McNulty SN, Cimino PJ, Cottrell CE, Heusel JW, Vigh-Conrad KA and Duncavage EJ: Targeted next-generation sequencing in molecular subtyping of lower-grade diffuse gliomas: Application of the World Health Organization's 2016 revised criteria for central nervous system tumors. J Mol Diagn *19(2)*: 328-337, 2017. PMID: 28042970. DOI: 10.1016/j.jmoldx.2016.10.010
23 Padul V, Epari S, Moiyadi A, Shetty P and Shirsat NV: ETV/Pea3 family transcription factor-encoding genes are overexpressed in *CIC*-mutant oligodendrogliomas. Genes Chromosomes Cancer *54(12)*: 725-733, 2015. PMID: 26357005. DOI: 10.1002/gcc.22283
24 McNamara MG, Jiang H, Lim-Fat MJ, Sahebjam S, Kiehl T-R, Karamchandani J, Coire C, Chung C, Millar B-A, Laperriere N and Mason WP: Treatment outcomes in 1p19q co-deleted/partially deleted gliomas. Can J Neurol Sci *44(3)*: 288-294, 2017. PMID: 28488951. DOI: 10.1017/cjn.2016.420
25 Na K, Kim HS, Shim HS, Chang JH, Kang SG, Kim SH. Targeted next-generation sequencing panel (TruSight Tumor 170) in diffuse glioma: a single institutional experience of 135 cases. J Neurooncol *142(3)*: 445-454, 2019. PMID: 30710203. DOI: 10.1007/s11060-019-03114-1
26 Nauen D, Haley L, Lin MT, Perry A, Giannini C, Burger PC and Rodriguez FJ: Molecular analysis of pediatric oligodendrogliomas highlights genetic differences with adult counterparts and other pediatric gliomas. Brain Pathol *26(2)*: 206-214, 2016. PMID: 26206478. DOI: 10.1111/bpa.12291
27 Hassanudin SA, Ponnampalam SN and Amini MN: Determination of genetic aberrations and novel transcripts involved in the pathogenesis of oligodendroglioma using array comparative genomic hybridization and next generation sequencing. Oncol Lett *17(2)*: 1675-1687, 2019. PMID: 30675227. DOI: 10.3892/ol.2018.9811
28 Zhang T, Guzman MA, Batanian JR. Narrowing down the common cytogenetic deletion 14q to a 5.6-Mb critical region in 1p/19q codeletion oligodendroglioma-relapsed patients points to two potential relapse-related genes: *SEL1L* and *STON2*. Cytogenet Genome Res *160(6)*: 316-320, 2020. PMID: 32575107. DOI: 10.1159/000509020

Received January 3, 2021
Revised January 22, 2021
Accepted January 25, 2021